Costimulatory action of glycoinositolphospholipids from *Trypanosoma cruzi:* increased interleukin 2 secretion and induction of nuclear translocation of the nuclear factor of activated T cells 1

MARIA BELLIO,[1] ANA-CAROLINA S. C. OLIVEIRA, CLAUDIA S. MERMELSTEIN,* MARCIA A. M. CAPELLA,[†] JOÃO P. B. VIOLA,[‡] JEAN-PIERRE LEVRAUD,[§] GEORGE A. DOSREIS,[†] JOSÉ O. PREVIATO, AND LUCIA MENDONÇA-PREVIATO

Instituto de Microbiologia Prof. Paulo de Goes, *Departamento de Histologia e Embriologia, ICB, [†]Instituto de Biofísica Carlos Chagas F°, Universidade Federal do Rio de Janeiro, 21.941–590 Rio de Janeiro, RJ, Brazil; [‡]Programa de Medicina Experimental, Instituto Nacional do Cancer, Rio de Janeiro, RJ, Brazil; and [§]Unité INSERM U 277, Institut Pasteur, 75724 Paris Cedex 15, France

ABSTRACT **The effects of the glycoinositolphospholipids (GIPLs) from *Trypanosoma cruzi* on T lymphocyte activation were investigated in a mouse T cell hybridoma (DO-11.10). Purified GIPLs from *T. cruzi* strains Y and G markedly increased IL-2 mRNA transcripts and IL-2 secretion induced by mitogenic anti-CD3 and anti-Thy1 mAbs. This costimulatory function was also revealed by the induction of IL-2 secretion after the simultaneous addition of the *T. cruzi* GIPLs and either the calcium ionophore A23187 or phorbol ester. The capacity of the GIPL molecule to induce an increase in cytoplasmic calcium levels was also demonstrated. After exposure of T cell hybridoma to GIPL, the nuclear transcription factor NFAT1 became partially dephosphorylated, and its nuclear localization was demonstrated both in the T cell hybridoma and in Balb/c $CD3^+$ cells. These results demonstrate that *T. cruzi* GIPL molecules are capable of signaling to T cells and therefore could be valuable tools for the study of T cell activation, besides playing a potential role in subverting the T lymphocyte immune response during *T. cruzi* infection.—Bellio, M., Oliveira, A.-C. S. C., Mermelstein, C. S., Capella, M. A. M., Viola, J. P. B., Levraud, J.-P., Dosreis, G. A., Previato, J. O., Mendonça-Previato, L. Costimulatory action of glycoinositolphospholipids from *Trypanosoma cruzi:* increased interleukin 2 secretion and induction of nuclear translocation of the nuclear factor of activated T cells 1. *FASEB J.* 13, 1627–1636 (1999)**

Key Words: T cell activation · ceramide · costimulation · Chagas' disease · cytosolic calcium

THE PROTOZOAN PARASITE *Trypanosoma cruzi* is the causative agent of Chagas' disease, which is endemic in Latin America. The surface of trypanosomatid parasites contains large amounts of glycoinositolphospholipids (GIPLs),[2] which occur either as glycosylphosphatidylinositol (GPI) anchors for glycoproteins and polysaccharides or as free GIPLs, which contain the same core structure of GPI (1). The oligosaccharide sequences and lipid structure of the major GIPLs from both the Y and G strains of *T. cruzi* were recently resolved by nuclear magnetic resonance (NMR) spectroscopy and fast atom bombardment mass spectrometry techniques (2–4).

These GPI family molecules from pathogenic protozoan parasites could play important roles in the establishment of chronic parasitic infections. GPI molecules from the malaria parasite activate signal transduction pathways in the host immune system, resulting in secretion of the proinflammatory cytokine tumor necrosis factor α (TNF-α) (5). Lipophosphoglycan from *Leishmania*, on the other hand, is a protein kinase C (PKC) -inhibitory molecule that is able to deactivate human monocytes and block their ability to undergo a respiratory burst (6, 7). In the presence of the host cytokine interferon γ (IFN-γ),

[1] Correspondence: Depto. de Imunologia/Instituto de Microbiologia Prof. Paulo de Goes, CCS Bl. I - 2° andar Sala: I2–053, UFRJ -Cidade Universitaria, CEP: 21941–590 Ilha do Fundao, Rio de Janeiro, RJ. Brazil. E-mail: belliom@acd.ufrj.br

[2] Abbreviations: CsA, cyclosporin A; DAG, 1,2 diacylglycerol; FCS, fetal calf serum; GIPL, glycoinositolphospholipid; GPI, glycosylphosphatidylinositol; IFN, interferon; Ig, immunoglobulin; IL, interleukin; mAb, monoclonal antibody; NAFT1, nuclear factor of activated T cells 1; NMR, nuclear magnetic resonance; PBS, phosphate-buffered saline; PCR, polymerase chain reaction; PKC, protein kinase C; PMA, phorbol 12-myristate 13-acetate; RT-PCR, reverse transcriptase-polymerase chain reaction; SDS-PAGE, sodium dodecyl sulfate-polyacrylamide gel electrophoresis; SPP, sphingosine 1-phosphate; TCR, T cell receptor; TNF, tumor necrosis factor.

however, lipophosphoglycan exacerbates host macrophage nitric oxide secretion (8), suggesting an opposing effect at later stages of infection. GIPLs from *T. cruzi* down-regulate host T cell activation through their ceramide domain (9), while augmenting B cell activation and immunoglobulin (Ig) secretion through their glycan chain (10). Moreover, GPI-anchored mucin-like glycoproteins isolated from *T. cruzi* induce interleukin 12 (IL-12) and TNF-α synthesis by macrophages (11, 12). The GPI moiety of the mucin-like glycoproteins is both sufficient and necessary to trigger proinflamatory cytokine production (12). Therefore, both agonist and antagonist signal-transducing actions on the host immune system can be mediated by parasite-derived GPI molecules. Although GIPLs are the most abundant glycoconjugates expressed on the surface of *T. cruzi*, the nature of the molecular events triggered by this class of parasite molecules in the cells of the host immune system remains largely unclear.

In the present study we investigate the molecular effects of *T. cruzi* GIPLs on signal transduction by a hybridoma T cell line. We demonstrate that Y and G strain GIPL potentiate both CD3 and Thy1-mediated IL-2 secretion, as well as IL-2 mRNA accumulation. *T. cruzi* GIPL induces a rise in free $[Ca^{2+}]_i$ in T cells, an effect that was mapped to the GIPL ceramide moiety. Moreover, *T. cruzi* GIPL, by itself, induces the dephosphorylation of the nuclear factor of activated T cells 1 (NFAT1) and its translocation to the nucleus, both in the T cell hybridoma and in freshly isolated mouse spleen T cells, through a cyclosporin A (CsA) -sensitive mechanism. These results demonstrate that *T. cruzi*-derived GIPLs interfere with signal transduction in host T cells, a finding that could have implications for the immunological alterations induced by *T. cruzi* infection.

MATERIALS AND METHODS

Isolation and purification of trypanosomatid GIPLs and their sugar and lipid components

The procedure was the same as described previously (2). Briefly, epimastigotes of *T. cruzi* (G and Y strains) and *Phytomonas serpens* were grown in BHI-hemin medium supplemented with 5% fetal calf serum (FCS). At early stationary growing phase (5 d at 26°C, with shaking), cells were harvested, washed three times with 0.9% NaCl, and stored frozen. Cells were thawed and extracted three times with cold water, centrifuged (7000 × *g*, 10 min), and the remaining cell pellet was extracted with 45% aqueous phenol at 75°C, 15 min. The aqueous layer from phenol extraction was dialyzed, freeze-dried, dissolved in water, and applied to a column of Bio-Gel P-100. The excluded material was lyophilized and the GIPLs were extracted by chloroform/methanol/water (10:10:3). The purified GIPL could be dissolved in water and sterile-filtered for use in tissue culture. The GIPL appeared on sodium dodecyl sulfate-polyacrylamide gel electrophoresis (SDS-PAGE) as a fast-moving, single molecular species. Virtual absence of contaminating peptidic material was confirmed by absence of peptide-derived signals in NMR analysis of the purified material (4). For isolation of phosphoinositol oligosaccharides and the lipid moiety, the intact GIPL was subjected to alkaline hydrolysis (1M KOH, for 48 h at 37°C) (13). After neutralization with acetic acid, nonpolar material from G strain GIPL, comprising a ceramide, was obtained by chloroform extraction, purified by silica chromatography, and evaporated to dryness. The ceramide was dissolved in phosphate-buffered saline (PBS) containing 10% ethanol, by heating at 60–90°C, to a stock concentration of 500 μg/ml. The ceramide domain was characterized as *N*-lignoceroylsphinganine by gas chromatography/mass spectrometry (2, 4).

Cells and reagents

DO-11.10 cells (14) were grown in complete 10% FCS RPMI 1640 (Gibco, Grand Island, N.Y.). Splenic T cells were isolated from normal male 4 wk old Balb/c mice by nylon wool filtration; CsA was from Sandoz Inc. (East Hanover, N.J.).

Activation and IL-2 assays

DO-11.10 cells were washed in serum-free medium and resuspended in 1% v/v Nutridoma-SR (Boehringer Mannheim, Mannheim, Germany) RPMI 1640. 10^5 cells/well were added to 96-well plates (Falcon, Oxnard, Calif.) with or without immobilized 145–2C11 (anti-CD3) or soluble G7 (anti-Thy1) monoclonal antibodies (mAbs) at the indicated concentrations. Alternatively, DO-11.10 cells were stimulated with phorbol 12-myristate 13-acetate (PMA) (Sigma, St. Louis, Mo.) and/or the calcium ionophore A23187 (Sigma) at the indicated doses. Supernatants were collected 20 to 24 h later. For IL-2 assay, 10^4 CTLL-2 cells per well were cultured in 100 μl of medium containing 20% of conditioned supernatants or different doses of rIL-2 in 96-well microculture plates (Costar, Cambridge, Mass.). Proliferation was assessed by ^{3}H-thymidine (Amersham, Amersham, U.K.) incorporation (0.5 μCi/well) and, for some experiments, IL-2 units were estimated as described previously (15). Results are shown as mean of triplicate cultures. The standard errors were within 10% of the mean.

PCR conditions and quantification of HPRT and IL-2 transcripts

All polymerase chain reactions (PCR) were performed in a Geneamp 9600 thermocycler (Perkin-Elmer, Norwalk, Conn.). PCR was performed in 20 μl volumes. The reaction mixture for PCR contained 0.2 mM each dNTP, 0.5 μM each primer, 2.5 mM $MgCl_2$, variable amounts of cDNA, 25 U/ml of Goldstar *Taq* DNA polymerase (Eurogentec, Seraing, Belgium), and the provided buffer. Reaction cycles consisted in 25 s at 94°C, 25 s at 60°C, and 30 s at 72°C. Cycles were preceded by 3 min of denaturation at 94°C, followed by 5 min of elongation at 72°C. Primer pairs for amplification of endogenous IL-2 and HPRT are described in ref 16 (the 5′ and run-off primers were used). Relative levels of HPRT and IL-2 transcripts were measured in the different cDNAs by PCR stopped in the exponential phase (17, 18). One of the two primers used being labeled with a FAM fluorophore, the amount of amplified product could be quantified after loading of 2 μl of PCR product diluted fourfold with formamide in a 373A automated DNA sequencer (Applied Biosystems). The products were loaded along size standards and the data were analyzed with Immunoscope software (19). The number

TABLE 1. *Increase in T cell IL-2 secretion induced by T. cruzi GIPL*[a]

Experiment	Treatment	Dose	GIPL[b]	IL-2 (units/ml)
1	None	—	+	N.D.[c]
	Anti-CD3	3.75 μg/ml	−	31.0
			+	177.0
	Anti-CD3	15.0 μg/ml	−	126.0
			+	>228.0
2	None	—	+	N.D.
	Anti-Thy1	2.5%[d]	−	2.4
			+	21.3
	Anti-Thy1	10%	−	22.2
			+	50.4
3	Anti-Thy1	10%	−	13.3
			+GIPL ceramide[e]	35.4
			+GIPL glycan[f]	15.5

[a] DO-11.10 cells were stimulated by either anti-CD3 mAb (2C11) immobilized on tissue culture microplates or soluble anti-Thy1 mAb (G7). [b] G strain, added at 25 μM. [c] Not detectable. [d] Final dilution (v/v) of G7 culture supernatant. [e] GIPL ceramide portion, added at 25 μM. [f] GIPL glycan portion added at 25 μM.

of cycles that provided sufficient signal without leaving the exponential phase was first assessed in a preliminary kinetic experiment. Typically, 22 cycles were required for HPRT, 30 for IL-2. For each sample, four tubes were amplified in each reaction, containing decreasing volumes of cDNA as initial template. That the final signal decreased proportionally to the initial amount of template was used as a control that the amplification was stopped in the exponential phase.

Immunofluorescence microscopy

Cells were placed on poly-D-lysine (Sigma) coated glass slides for 30 min, stimulated or not by the indicated treatments, and fixed with 4% formaldehyde in PBS for 15 min at room temperature. They were then permeabilized and blocked by washing four times with 0.5% Triton-X 100 (Sigma), 5% FCS, 0.01% Na azide in PBS for 5 min. This PBS/FCS/Triton/Na azide solution was also used for all subsequent washing steps. Primary antibodies anti-CD3 (145–2C11, FITC-labeled, PharMingen, San Diego, Calif.) and anti-NFAT1 (20) (anti-67.1 antibody, a rabbit polyclonal antibody to the 67.1 peptide in the amino-terminal region of NFAT1, a kind gift of Dr. A. Rao, Harvard Medical School, Boston), used at appropriate dilution, were incubated for 1 h at 37°C and washed three times for 10 min each. Secondary goat anti-rabbit antibody (Sigma) was tagged with rhodamine, incubated at 1:400 dilution for 1 h at 37°C, and washed three times for 10 min each. The nuclear dye DAPI (4, 6-diamidino-2-phenylindole dihydrochloride; Polysciences, Warrington, Pa.) was used at 0.2 mg/ml in 0.9% NaCl for 5 min at room temperature. Specimens were mounted in glycerol containing, by weight, 5% n-propyl gallate (Sigma), 0.25% DABCO (1, 4-diazabicyclo (2, 2, 2) octane, Sigma), and 0.0025% para-phenylenediamine (Sigma). Cells were examined with an Axiovert 100 epifluorescence microscope (Carl Zeiss), using filter sets that were selective for rhodamine, fluorescein, or the blue wavelength channel. Differential interference contrast microscopy (DIC) was performed on the same microscope. Images were acquired with a C2400i integrated CCD camera (Hamamatsu Photonics) using Argus 20 image processor (Hamamatsu Photonics). Digitized images were transferred to a Dell OptiPlex GL 575 computer (Dell Computer Corporation) and further improved with Adobe Photoshop (Adobe Systems) in a Quadra 840AV Macintosh computer (Apple). Photographs of processed images were made directly from the monitor screen, using 125 ASA Plus-X pan film (Eastman Kodak). Control experiments with no primary antibodies showed only a faint background staining (not shown).

SDS whole cells lysates and Western blotting

After the various treatments, the cells (1.5×10^6/lane) were resuspended in 20 μl of buffer (40 mM Tris, pH 8, 60 mM pyrophosphate, and 10 mM EDTA) and lysed by addition of equal volume of 10% SDS, followed by boiling for 20 min in reducing sample buffer. The lysates were analyzed by 7% SDS-PAGE, followed by Western blotting with anti-NFAT1 (20) (anti-67.1 antibody) and secondary anti-rabbit IgG horseradish peroxide-labeled antibody (Santa Cruz Biotechnology, Santa Cruz, Calif.). The bands were visualized using enhanced chemiluminescence (Amersham). Films were scanned in a Umax UC1260 scanner and optical density measurements made by the NIH Image software.

Measurement of cytosolic calcium

Cells were loaded with 6 μM Fura 2-AM (Molecular Probes, Eugene, Oreg.) for 30 min at 37°C and washed three times with PBS for complete removal of the dye. After washing, cells were incubated in PBS (1 mM Ca^{2+}, 1 mM Mg^{2+}) for 5 min in a petri dish mounted with a glass coverslip. Calcium measurements were performed in an inverted microscope equipped with a digital ratio imaging system (Attofluor, Zeiss), with excitation at 334 nm and 380 nm and emission measured with a 520 nm long pass filter.

RESULTS

Costimulatory effect of *T. cruzi* GIPL on IL-2 production

GIPLs purified from *T. cruzi* strains Y or G were added to cultures of the T hybridoma cell line

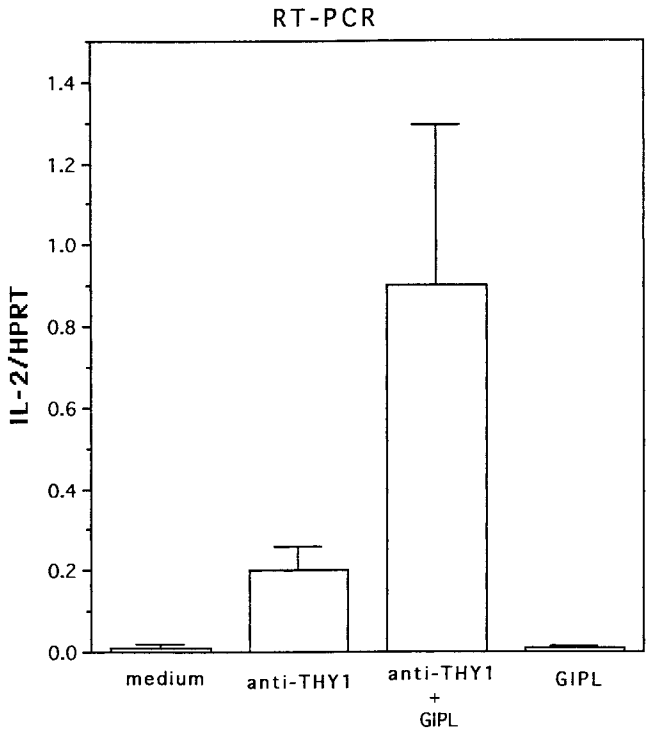

Figure 1. Semiquantitative analysis of IL-2 mRNA by RT-PCR. DO-11.10 cells (5×10^6 cells/ml) were stimulated in RPMI 1% Nutridoma, with 2.0% final dilution (v/v) of G7 (anti-Thy1) culture supernatant in the presence or absence of 25 μM of GIPL, as indicated. RNA was extracted 8 h later and RT-PCR was performed as described in Materials and Methods.

DO-11.10 stimulated or not with mitogenic antibodies (anti-CD3 or anti-Thy1). The IL-2 production assays in two representative experiments with G strain GIPL are shown in **Table 1**. The amount of secreted IL-2 is increased by more than fivefold or higher when suboptimal mAbs doses are used and the costimulatory effect of GIPL can be observed even with saturating doses of anti-CD3 or anti-Thy1 mAbs. The purified GIPL ceramide and glycan domains were added separately at equimolar concentrations to anti-Thy1-treated cultures (Table 1, exp. 3), mapping the biological activity of *T. cruzi* GIPL to its ceramide domain. Similar results were obtained with Y strain GIPL, which has the same lipid but different glycan moieties (2); no effect was observed using GIPLs obtained from a plant trypanosomatid (*Phytomonas serpens*), which differ both in lipid and glycan structures (21) and were purified by the same protocol as *T. cruzi* GIPLs (data not shown). Addition of GIPL in the absence of mitogenic mAbs induces little or no IL-2 secretion. The higher IL-2 secretion induced by GIPL in anti-Thy1-treated cultures was due to an increase in IL-2 mRNA content, since semiquantitative RT (reverse transcriptase)-PCR analysis showed that the addition of *T. cruzi* GIPL caused a rise in IL-2 mRNA levels (**Fig. 1**).

The costimulatory function of GIPL is not substituted for by PMA

Ceramides can activate the proto-oncogene Vav, which plays a critical role in T cell receptor (TCR) -mediated cell activation and has a lipid binding domain that recognizes phorbol ester and 1,2 diacylglycerol (DAG) (22). Although a number of enzymes bind either ceramide or DAG, opposing and antagonizing effects of these second messengers have also been described (23, 24). Therefore, the effects of the addition of phorbol ester (a PKC activator) on the costimulatory function of *T. cruzi* GIPL were evaluated in our system. **Figure 2** shows the dose-effect curve of the addition of *T. cruzi* GIPL to DO-11.10 cells stimulated by anti-Thy1 (G7) mAb in the presence or absence of PMA. GIPL addition led to a significant increase in IL-2 production regardless of the presence of PMA. However, PMA treatment markedly increased the potency of GIPL effects, resulting in an ED_{50} of 1.1 μM GIPL compared to 10.8 μM GIPL in the absence of PMA. Similar results were seen at higher G7 mAb concentrations, although the synergism between PMA and GIPL was less intense (not shown). This result suggests that GIPL and PMA signaling to the T cell are independent.

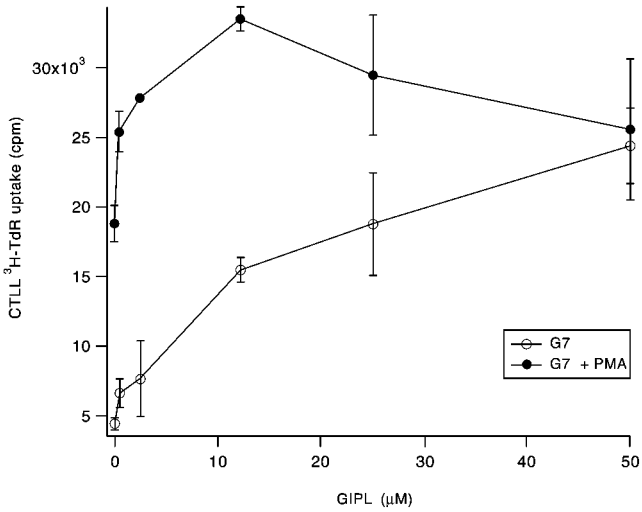

Figure 2. Dose response of GIPL effect on IL-2 production. DO-11.10 cells were stimulated with 2.0% final dilution (v/v) of G7 (anti-Thy1) culture supernatant, in the presence of the indicated doses of G strain GIPL. PMA was added (closed symbols) or not (open symbols) at a final concentration of 10 ng/ml.

TABLE 2. *Synergism between T. cruzi G strain GIPL and PMA or calcium ionophore*[a]

Experiment	Stimulus (dose)	IL-2 (units/ml)
		N.D[b]
1	GIPL (50.0 μM)	
	PMA (20.0 ng/ml)	N.D
	GIPL (50.0 μM) + PMA (20.0 ng/ml)	11.7
2	GIPL (5.0 μM)	N.D
	GIPL (50.0 μM)	1.0
	PMA (10.0 ng/ml)	1.1
	PMA (10.0 ng/ml) + GIPL (50.0 μM)	16.6
	A23187 (0.5 μg/ml)	20.7
	A23187 (0.5 μg/ml) + GIPL (5.0 μM)	262.0
3	GIPL (5.0 μM)	N.D
	A23187 (0.05 μg/ml)	0.5
	A23187 (0.05 μg/ml) + GIPL (5.0 μM)	8.0

[a] DO-11.10 cells were cultured in RPMI 1640, 1% Nutridoma, with the indicated reagents for 20 h. Supernatants were collected and tested in CTLL-2 bioassays. [b] Not detectable.

GIPL synergizes independently with either PMA or calcium ionophore in IL-2 secretion

To test the hypothesis that GIPL would activate more than one signaling pathway in T cells, we studied its capacity to synergize with either PMA or A23187 in the absence of other stimuli. While PMA or GIPL added alone to the T hybridoma cultures induced little or no detectable IL-2 secretion, in their simultaneous presence significant levels of IL-2 could be found in supernatants (**Table 2**). On the other hand, the calcium ionophore A23187 at certain doses can stimulate IL-2 secretion by DO-11.10 cell; when added to cultures simultaneously

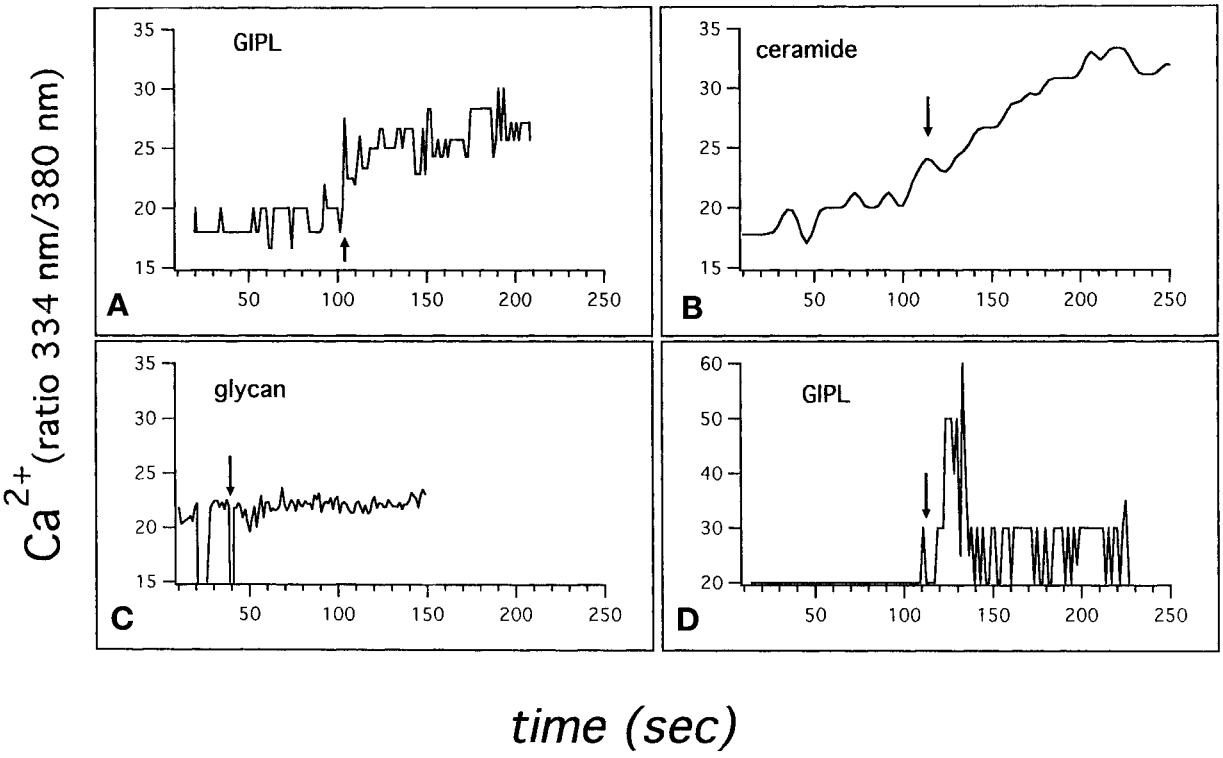

Figure 3. GIPL increases the cytosolic calcium concentration. Fura-2-loaded DO-11.10 cells were resuspended in PBS (1 mM Ca^{2+}) and analyzed for Ca^{2+} increase in an inverted microscope equipped with a digital ratio imaging system. Cells were treated with *A)* 50.0 μM of GIPL; *B)* 50.0 μM GIPL; derived ceramide; *C)* 50.0 μM of GIPL-derived glycan; *D)* 50.0 μM of GIPL. Arrows indicate when material was added. Averaging is used in panels *A*—*C*; in panel *D*, single cell measurement was done. Results are plotted as the ratio of the fluorescence emission of Fura-2/AM at 520 nm after alternating excitation at 334 nm/380 nm against time (s).

with GIPL, large amounts (more than a 10-fold increase) of IL-2 could be observed. As expected, PMA and calcium ionophore strongly synergized on IL-2 production, bypassing TCR signaling. The results suggest that GIPL can mimic either Ca^{2+} or PKC activation signals for T cell activation.

The cytosolic calcium concentration is increased by GIPL

The synergism between GIPL and PMA in IL-2 production suggested that GIPL could be inducing an increase of cytosolic calcium concentration. Therefore, we measured free $[Ca^{2+}]_i$ levels in T cells treated with GIPL (**Fig. 3**). Addition of 50.0 μM of GIPL to DO-11.10 cells induced a $[Ca^{2+}]_i$ increased response in seconds (Fig. 3*A*) and of a magnitude similar to the one obtained by the addition of PHA (10.0 μg/ml, data not shown). Purified ceramide and glycan moieties of GIPL were also tested for this biological effect. Figure 3*B, C* shows respectively, the effects on cytosolic calcium concentration induced by the addition of the purified ceramide or glycan portions of GIPL at stoichiometric doses of the intact molecule used in Fig. 3*A*. Only the ceramide moiety was able to induce elevation of $[Ca^{2+}]_i$ (Fig. 3*B*). The recording of a single cell response (Fig. 3*D*) demonstrates the characteristic oscillatory pattern of cytosolic-free calcium concentration induced by GIPL, a nearly universal mode of calcium signaling that was recently described to increase the efficiency and specificity of gene expression (25, 26).

The effect of GIPL on NFAT1 dephosphorylation

The effects of GIPL on the activation of the nuclear transcription factor NFAT1 were investigated by Western blot analysis of DO-11.10 cell extracts. It is known that the activation of NFAT1 is reflected by its dephosphorylation, which precedes nuclear translocation and is revealed as a faster electrophoretic mobility on SDS gels (27). Addition of G strain GIPL alone induced partial dephosphorylation of NFAT1 as shown in **Fig. 4**. The kinetics of NFAT1 dephosphorylation shows that it is detectable after 5 min and is maximal after 30 min of GIPL addition. We also know that NFAT1 is phosphorylated at multiple serine residues in resting cells and is progressively dephosphorylated in response to increasing levels of calcium concentration (27, 28). Figure 4*B* shows the NFAT1 dephosphorylation induced by increasing amounts of GIPL. Note the appearance of a partially dephosphorylated form after treatment with GIPL, migrating at 14 mm (Fig. 4*C*). The degree of NFAT1 dephosphorylation, however, is lower than that induced by the calcium ionophore A23187. In the experiment shown in Fig. 4*A*, the amount of total

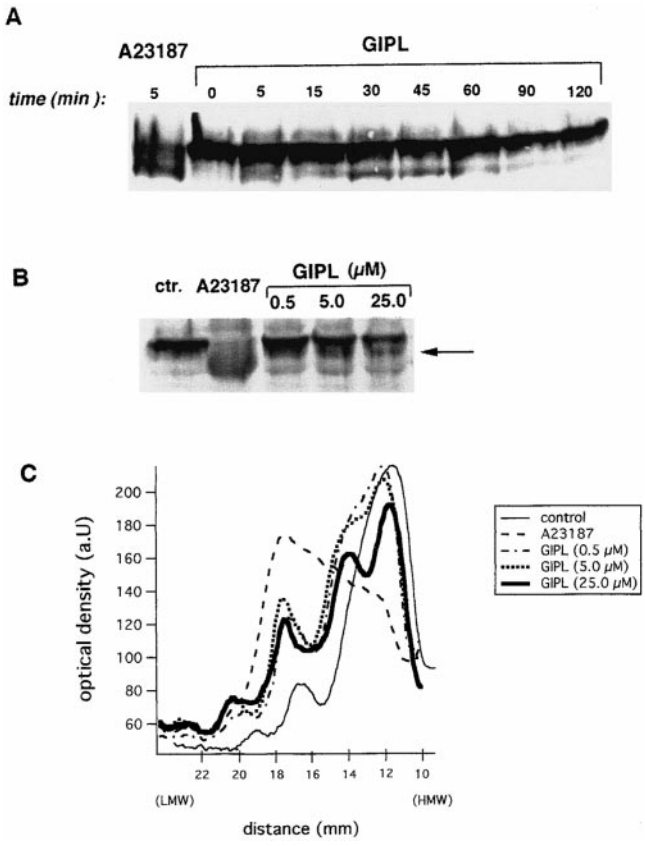

Figure 4. The effect of GIPL on NFAT1 dephosphorylation. Lysates were analyzed by 7% SDS-PAGE, followed by Western blotting with anti-NFAT1 (anti-67.1 antibody) and secondary anti-rabbit IgG-horseradish peroxide-labeled antibody. Bands were visualized using enhanced chemiluminescence. *A)* Kinetics. DO-11.10 cells (1×10^6) were stimulated for 5 min with 0.5 μg/ml of A23187 or for the times indicated with 25.0 μM of GIPL. *B)* Dose-dependent response. DO-11.10 cells (1×10^6) were stimulated for 15 min with 0.5 μg/ml of A23187 or with the indicated doses of GIPL. Arrow points to the intermediary dephosphorylated form of NFAT1. *C)* Densitometry (in arbitrary units) of results shown in panel *B* obtained using NIH Image software. LMW = low molecular weight, HMW = high molecular weight.

protein dephosphorylated by 5 min of A23187 treatment is 56%, whereas 41% of the NFAT1 is dephosphorylated by 30 min of treatment with GIPL. In the presence of EGTA, NFAT1 dephosphorylation by GIPL could not be detected (not shown), indicating the calcium requirement for the activation of the phosphatase involved in the reaction.

The *T. cruzi* GIPL can induce NFAT1 nuclear translocation in Balb/c T lymphocytes

The subcellular localization of NFAT1 was assessed first in DO-11.10 cells by fluorescence microscopy with an NFAT1-specific antibody. **Figure 5** shows NFAT1 in the cytoplasm of unstimulated DO-11.10 cells (Fig. 5*A*) and its nuclear translocation after the cells have been treated for 30 min with 25.0 μM of

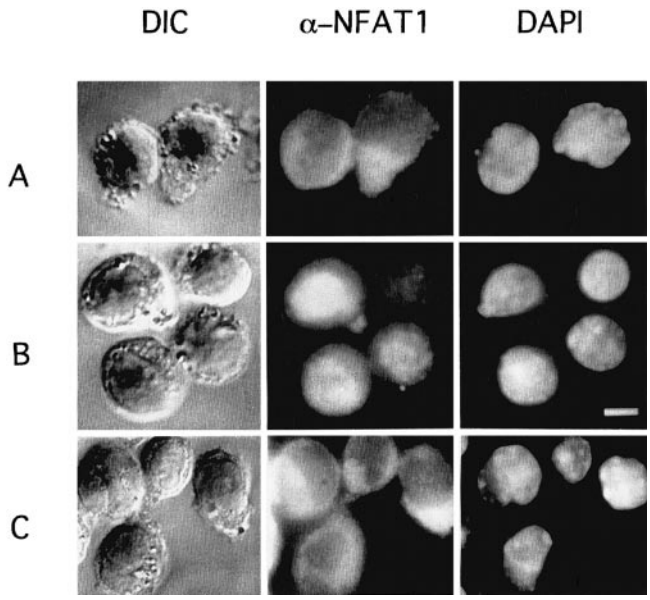

Figure 5. GIPL induces NFAT1 nuclear translocation in DO-11.10 cells. Cells were either left untreated (*A*) or treated with 50.0 μM of GIPL (*B*) or 50.0 μM of GIPL plus 1.0 μM of CsA (*C*) for 30 min. The differential interference contrast (DIC) microscopy and the fluorescence at the rhodamine (NFAT-1) and blue (DAPI) wavelength channels are shown. Bar = 5.0 μM.

GIPL (Fig. 5*B*). On the other hand, the majority of NFAT1 protein remains in the cytoplasm of cells treated with GIPL in the presence of CsA (Fig. 5*C*). Moreover, the purified ceramide moiety of GIPL (but not the molecule glycan domain) was able to induce NFAT1 nuclear translocation (data not shown). However, in contrast to the results obtained with the calcium ionophore, where we could observe NFAT1 translocation in every cell treated, the response to GIPL (or GIPL-derived ceramide) was not homogenous. Finally, the action of *T. cruzi* GIPLs on NFAT1 nuclear translocation was also investigated in freshly isolated T cells from Balb/c mice. Splenocytes were enriched for T lymphocytes by nylon wool filtration and left untreated (**Fig. 6 *A***) or stimulated with GIPL (Fig. 6*B*) or GIPL plus CsA (Fig. 6*C*). Again, the GIPL treatment induced nuclear translocation of NFAT1, which was CsA sensitive.

DISCUSSION

In the present study we described the costimulatory function of GIPLs purified from strains Y and G of *T. cruzi,* in T cell activation. The capacity of GIPL to induce up to 10-fold increase in IL-2 production by anti-CD3 or anti-Thy1 mAbs (Table 1) was reflected by the elevation of IL-2 mRNA levels (Fig. 1). This effect can be due to either an increase in IL-2 transcription or a post-transcriptional action increasing mRNA stability, as described previously for the CD28-mediated costimulatory pathway (29). This costimulatory action on IL-2 secretion by a T cell hybridoma was mapped to the ceramide domain of the GIPL molecule (Table 1), in accordance with a previous work where *T. cruzi* GIPL activity on murine T cells was investigated (9). Boucher et al. (30) and Chan and Ochi (31) have shown that the sphingomyelin-ceramide pathway was triggered after CD28-mediated signaling in T lymphocytes. Moreover, IL-1β binding to the 80 kDa IL-1 receptor also triggers the sphingomyelin pathway (32), and the costimulatory action of IL-1β on signaling for IL-2 production can be substituted by synthetic ceramide on EL4 cells (33). Therefore, ceramides appear to be involved in costimulatory effects on T cells, and the parasite GIPL mimics these effects by virtue of its ceramide domain.

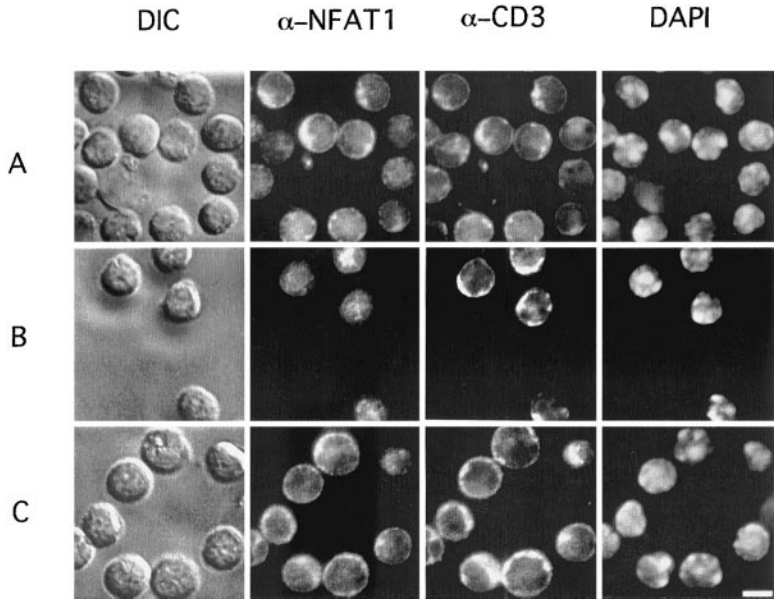

Figure 6. GIPL induces NFAT1 nuclear translocation in Balb/c T lymphocytes. Spleen $CD3^+$ cells were purified and either left untreated (*A*) or treated with 50.0 μM of GIPL (*B*) or 50.0 μM of GIPL plus 1.0 μM of CsA (*C*) for 30 min. The differential interference contrast (DIC) microscopy and fluorescence at the rhodamine (NFAT-1), fluorescein (anti-CD3), and blue (DAPI) wavelength channels are shown. Bar = 5.0 μM.

To further investigate the mode of GIPL action, we studied its possible interactions with PMA and the calcium ionophore A23187. The synergism between GIPL and either PMA or A23187 on IL-2 secretion (Table 2) indicates that GIPL may have multiple effects on cell signaling. The GIPL-induced dephosphorylation of NFAT1 (Fig. 4) is of lower magnitude than the one caused by A23187 treatment. This correlates with the finding that NFAT1 does not translocate to the nucleus in every GIPL-treated cell; the heterogeneity of this response is under investigation. GIPL by itself is not capable of inducing IL-2 secretion in the absence of another stimulus (Tables 1 and 2), although it induces NFAT1 dephosphorylation (Fig. 4) and NFAT1 nuclear translocation (Figs. 5 and 6). In fact, it has been shown that substantial fraction of NFAT1 localizes to the nucleus under conditions of only minor dephosphorylation (34). According to the model proposed by Beals et al. (34), a minimal level of dephosphorylation exposes the nuclear localization signal of the NFAT1 protein, bringing about a conformational change that may be required for additional functions such as DNA binding and *trans*-activation. Moreover, the IL-2 promoter is strongly synergistic and its activation reflects the convergence of multiple signal transduction pathways (reviewed in ref 35). In addition to NFAT, at least three other unrelated transcription factors are required for IL-2 gene expression: Oct, AP-1, and NF-κB. The simplest interpretation for the results obtained would be that the GIPL molecule is unable to induce the activation (at the required levels) of at least one of the transcription factors needed and that this factor would be activated by either PMA or A23187. Alternatively, the activation of the transcription factors itself can be dependent on the synergistic action of different second messengers. An example is the activation of JNK, the kinase that mediates *trans*-activation of c-Jun, one of the AP-1 components. TCR/CD3 and CD28 costimulation synergistically activates JNK and can be substituted by the combined treatment with PMA and calcium ionophore for optimal JNK activation (36). Therefore, the possibility that the GIPL molecules are also inducing the activation of other nuclear factors, perhaps in synergism with PMA or A23187, requires further investigation. Of particular interest would be the investigation of the effects of *T. cruzi* GIPL on AP-1, since sphingolipid-derived messengers were found to engage the MAPK cascade (37). Preliminary results indicate that NF-κB translocates to the nucleus in DO-11.10 cells treated with GIPL alone (data not shown). Accordingly, NF-κB activation by ceramides, although controversial (38), has been described (39–41), including in CD28 signaling (30, 31). On the other hand, even though the CD28 pathway of NFAT1 activation is known to have a component that is CsA insensitive (42), in our experiments CsA abrogated NFAT1 translocation.

Ceramide has recently emerged as a pleiotropic biological activator, involved in cellular activities, as divergent as cell proliferation and apoptosis. Several potential targets for this second messenger action have been designed (reviewed in refs 43, 44), and probably a complex pattern of integrated signals may arise in response to elevation of ceramide content in cells. Therefore, the differential expression of these targets in distinct cell types may explain the described disparate outcomes of ceramide action. This could account for the reduction in IL-2 secretion observed in cultures of freshly isolated T cells treated with *T. cruzi* GIPLs (10), in contrast to the results with a T cell hybridoma reported herein. Nevertheless, we do observe NFAT1 nuclear translocation in GIPL-treated splenic T lymphocytes (Fig. 6); other groups have also shown an increase in IL-2 and IL-4 mRNA levels in splenic T cells and T clones treated with C_6-ceramide or sphingosine, respectively (31, 45). An alternative explanation for the different outcomes in IL-2 production described here and in the previous study is that *T. cruzi* GIPLs are activating a suppressor T cell activity such as cytokines or a regulatory cell subset. It was recently reported that the addition of sphingosine to T cell cultures seems to preferentially affect Th2 cells (45).

In the present study, the capacity of *T. cruzi* GIPL and GIPL-derived ceramide (whose major component is a *N*-lignoceroyldihydrosphingosine) (2) to increase cytosolic calcium in T cells is shown for the first time (Fig. 3). This is in accordance with the CsA-sensitive nuclear translocation of NFAT1 also induced by *T. cruzi* GIPL (Figs. 5 and 6). The mechanisms regulating the calcium increase, however, need further investigation. Both sphingosine and sphingosine 1-phosphate (SPP) affect intracellular calcium in different cell types including Jurkat leukemia T cells (46), although each of these compounds seems to act through distinct mechanisms (reviewed in ref 37). An additional complication arises from the fact that sphingosine and SPP are metabolically interconvertible; moreover, sphingosine can be reacylated to ceramide (37). It is also noteworthy that C6, but not C2-ceramide, enhances cytoplasmic free Ca^{2+} in platelets (47), suggesting the dependence on *N*-acyl chain length of ceramide for its action. The relevance of $[Ca^{2+}]_i$ elevation and, more important, of its oscillatory pattern, in NFAT *trans*-activation has recently been described (25, 26). Also, an increase in cytosolic calcium is observed and appears to be required for nonphagocytic cell invasion by *T. cruzi* (48).

It would be interesting to study whether the added *T. cruzi* dihydroceramide can incorporate the 4,5-*trans*-double bound by entering the sphingolipid intermediary metabolism (49) and then be converted to sphingosine and sphingosine 1-phosphate.

Although in some systems synthetic dihidroceramides have no effect (37), it was demonstrated that the 4,5 double bound is not critical for the sphingosine-induced cell proliferation in 3T3 cells (50).

The costimulatory effects of *T. cruzi* GIPLs described here may play a role in the disturbances of the immune system observed in Chagas' disease. Evidence suggests the occurrence of GIPLs in infective and amastigote forms of *T. cruzi* (51, 52); in addition, a carbohydrate-containing antigen was detected in the sera of *T. cruzi*-infected mice (53). A fraction of this antigen contains fatty acids and phosphorus, and may correspond to the glycophospholipid molecule (54). The infection with *T. cruzi* causes a massive nonspecific polyclonal activation of host B and T lymphocytes, generating a state of general immunosuppression (55). However, little is known about the molecules causing this extensive activation. Moreover, it was recently shown that activation-induced $CD4^+$ T cell apoptosis is a prominent feature of experimental infection with *T. cruzi* (56). Although GIPL-derived ceramide cannot by itself induce programmed cell death in T cells (9) or in T hybridomas (data not shown), it triggers apoptosis in IFN-γ-treated macrophages (57) and in T lymphocytes from *T. cruzi*-infected mice (D. O. Nascimento and G. A. DosReis, unpublished observations). Therefore, these results justify a more detailed investigation on the immunopathogenic action of GIPLs *in vivo*, along with further studies of its putative action on other signaling pathways in T cells. FJ

We are indebted to Dr. Alberto F. A. Nobrega for the generous gift of reagents and for helpful discussions. We also thank Dr. Philippe Kourilsky for support and critical reading the manuscript, Dr. Anjana Rao for providing us the anti-NFAT1 antibody, and Drs. Adalberto Vieyra, Manoel L. Costa, and Ulisses Lopes for reagents and use of photo facilities. L.M-P is a Howard Hughes International Research Scholar. Grant support included CNPq, FINEP/PRONEX, FUJB, FAPERJ, HHMI, and CEPG/UFRJ.

REFERENCES

1. McConville, M., and Ferguson, M. A. J. (1993) The structure, biosynthesis and function of glycosylated phosphatidylinositols in the parasitic protozoa and higher eukaryotes. *Biochem. J.* **294,** 305–324
2. Previato, J. O., Gorin, P. A. J., Mazurek, M., Xavier, M. T., Fournet, B., Wieruszesk, J. M., and Mendonça-Previato, L. (1990) Primary structure of the oligosaccharide chain of lipopeptidophosphoglycan of epimastigote forms of *Trypanosoma cruzi*. *J. Biol. Chem.* **265,** 2518–2526
3. de Lederkremer, R. M., Lima, C., Ramirez, M. I., Ferguson, M. A., Homans, S. W., and Thomas-Oates, J. (1991) Complete structure of the glycan of lipopeptidophosphoglycan from *Trypanosoma cruzi* epimastigotes. *J. Biol. Chem.* **266,** 23670–23675
4. Carreira, J. C., Jones, C., Wait, R., Previato, J. O., and Mendonça Previato, L. (1996) Structural variation in the glycoinositolphospholipids of different strains of *Trypanosoma cruzi*. *Glycoconj. J.* **13,** 955–966
5. Schofield, L., and Hackett, F. (1993) Signal transduction in host cells by a glycosylphosphatidylinositol toxin of malaria parasites. *J. Exp. Med.* **177,** 145–153
6. Descoteaux, A., Turco, S. J., Sacks, D. L., and Matlashewski, G. (1991) *Leishmania donovani* lipophosphoglycan selectively inhibits signal transduction in macrophages. *J. Immunol.* **146,** 2747–2753
7. McNeely, T. B., and Turco, S. J. (1990) Requirement of lipophosphoglycan for intracellular survival of *Leishmania donovani* within human monocytes. *J. Immunol.* **144,** 2745–2750
8. Proudfoot, L., Nikolaev, A. V., Feng, G., Wei, X., Ferguson, M. A. J., Brimacombe, J. S., and Liew, F. Y. (1996) Regulation of the expression of nitric oxide synthase and leishmanicidial activity by glycoconjugates of *Leishmania* lipophosphoglycan in murine macrophages. *Proc. Natl. Acad. Sci. USA* **93,** 10984–10988
9. Gomes, N. A., Previato, J. O., Zingales, B., Mendonça-Previato, L., and DosReis, G. A. (1996) Down-regulation of T lymphocyte activation *in vitro* and *in vivo* induced by glycoinositolphospholipids from *Trypanosoma cruzi*. Assignment of the T cell-suppressive determinant to the ceramide domain. *J. Immunol* **156,** 628–635
10. Bento, C. A., Melo, M. B., Previato, J. O., Mendonça Previato, L., and Peçanha, L. M. (1996) Glycoinositolphospholipids purified from *Trypanosoma cruzi* stimulate Ig production *in vitro*. *J. Immunol.* **157,** 4996–5001
11. Camargo, M. M., Andrade, A. C., Almeida, I. C., Travassos, L. R., and Gazzinelli, R. T. (1997) Glycoconjugates isolated from *Trypanosoma cruzi* but not from *Leishmania* species membranes trigger nitric oxide synthesis as well as microbicidal activity in IFN-gamma-primed macrophages. *J. Immunol.* **159,** 6131–6139
12. Gazzinelli, R. T., Camargo, M. M., Almeida, I. C., Morita, Y. S., Giraldo, M., Acosta Serrano, A., Hieny, S., Englund, P. T., Ferguson, M. A., Travassos, L. R., and Sher, A. (1997) Identification and characterization of protozoan products that trigger the synthesis of IL-12 by inflammatory macrophages. *Chem. Immunol* **68,** 136–152
13. Smith, S. W., and Lester, R. L. (1974) Inositol phosphorylceramide, a novel substance and the chief member of a major group of yeast sphingolipids containing a single inositol phosphate. *J. Biol. Chem.* **249,** 3395–3405
14. Yague, J., White, J., Coleclough, C., Kappler, J., Palmer, E., and Marrack, P. (1985) The T cell receptor: the alpha and beta chains define idiotype, and antigen and MHC specificity. *Cell* **42,** 81–87
15. Kappler, J. W., and Marrack, P. (1986) Lymphokines. In *Handbook of Experimental Immunology* (Weir, O. M., ed) Vol. 2, Alden Press, Oxford, U.K.
16. Delassus, S., Coutinho, G. C., Saucier, C., Darche, S., and Kourilsky, P. (1994) Differential cytokine expression in maternal blood and placenta during murine gestation. *J. Immunol.* **152,** 2411–2420
17. Chelly, J., Montarras, D., Pinset, C., Berwald-Netter, Y., Kaplan, J. C., and Kahn, A. (1990) Quantitative estimation of minor mRNAs by cDNA-polymerase chain reaction. Application to dystrophin mRNA in cultured myogenic and brain cells. *Eur. J. Biochem.* **187,** 691–698
18. Azuara, V., Levraud, J.-P., Lembezat, M.-P., and Pereira, P. (1997) A novel subset of adult γδ thymocytes secreting a distinct pattern of cytokines and expressing a very restricted T cell receptor repertoire. *Eur. J. Immunol.* **27,** 544–553
19. Pannetier, C., Cochet, M., Darche, S., Casrouge, A., Zöller, M., and Kourilsky, P. (1993) The sizes of the CDR3 hypervariable regions of the murine T-cell receptor β chains vary as a function of the recombined germ-line segments. *Proc. Natl. Acad. Sci. USA* **90,** 4319–4323
20. Ho, A. M., Jain, J., Rao, A., and Hogan, P. G. (1994) Expression of the transcription factor NFATp in a neuronal cell line and in the murine nervous system. *J. Biol. Chem.* **269,** 28181–28186
21. Routier, F., Previato, J. O., Jones, C., Wait, R., and Mendonça-Previato, L. (1993) Glycoinositolphospholipids from members of the Trypanosomatidae family: investigation of the lipid moiety. *Ci. Cult. J. Braz. Assoc. Adv. Sci.* **45,** 66–68
22. Gulbins, E., Coggeshall, K. M., Baier, G., Telford, D., Langlet, C., Baier Bitterlich, G., Bonnefoy Berard, N., Burn, P., Wittinghofer, A., and Altman, A. (1994) Direct stimulation of Vav

guanine nucleotide exchange activity for Ras by phorbol esters and diglycerides. *Mol. Cell. Biol.* **14,** 4749–4758
23. Jarvis, W. D., Fornari, F. A., Jr., Browning, J. L., Gewirtz, D. A., Kolesnick, R. N., and Grant, S. (1994) Attenuation of ceramide-induced apoptosis by diglyceride in human myeloid leukemia cells. *J. Biol. Chem.* **269,** 31685–31692
24. Haimovitz Friedman, A., Kan, C. C., Ehleiter, D., Persaud, R. S., McLoughlin, M., Fuks, Z., and Kolesnick, R. N. (1994) Ionizing radiation acts on cellular membranes to generate ceramide and initiate apoptosis. *J. Exp. Med.* **180,** 525–535
25. Dolmetsch, R. E., Xu, K., and Lewis, R. S. (1998) Calcium oscillations increase the efficiency and specificity of gene expression. *Nature (London)* **392,** 933–936
26. Li, W., Llopis, J., Whitney, M., Zlokarnik, G., and Tsien, R. Y. (1998) Cell-permeant caged InsP3 ester shows that Ca^{2+} spike frequency can optimize gene expression. *Nature (London)* **392,** 936–941
27. Shaw, K. T. Y., Ho, A. M., Raghavan, A., Kim, J., Jain, J., Park, J., Sharma, S., Rao, A., and Hogan, P. G. (1995) Immunosuppressive drugs prevent a rapid dephosphorylation of transcription factor NFAT1 in stimulated immune cells. *Proc. Natl. Acad. Sci. USA* **92,** 11205–11209
28. Loh, C., Shaw, K. T. Y., Carew, J., Viola, J. P. B., Luo, C., Perrino, B. A., and Rao A. (1996) Calcineurin binds the transcription factor NFAT1 and reverse its activity. *J. Biol. Chem.* **271,** 10884–10891.
29. Umlauf, S. W., Beverly, B., Lantz, O., and Schwartz, R. H. (1995) Regulation of interleukin 2 gene expression by CD28 costimulation in mouse T-cell clones: both nuclear and cytoplasmic RNAs are regulated with complex kinetics. *Mol. Cell. Biol.* **15,** 3197–3205
30. Boucher, L. M., Wiegmann, K., Fütterer, A., Pfeffer, K., Machleidt, T., Schütze, S., Mak, T. W., and Krönke, M. (1995) CD28 signals through acidic sphingomyelinase. *J. Exp. Med.* **181,** 2059–2068
31. Chan, G., and Ochi, A. (1995) Sphingomyelin-ceramide turnover in CD28 costimulatory signaling. *Eur. J. Immunol.* **25,** 1999–2004
32. Ballou, L. R., Chao, C. P., Holness, M. A., Barker, S. C., and Raghow, R. (1992) Interleukin-1-mediated PGE2 production and sphingomyelin metabolism. Evidence for the regulation of cyclooxygenase gene expression by sphingosine and ceramide. *J. Biol. Chem.* **267,** 20044–20050
33. Mathias, S., Younes, A., Kan, C. C., Orlow, I., Joseph, C., and Kolesnick, R. N. (1993) Activation of the sphingomyelin signaling pathway in intact EL4 cells and in a cell-free system by IL-1 beta. *Science* **259,** 519–522
34. Beals, C. R., Clipstone, N. A., Ho, S. N., and Crabtree, G. R. (1997) Nuclear localization of NFATc by calcineurin-dependent, cyclosporin-sensitive intramolecular interaction. *Genes & Dev.* **11,** 824–834.
35. Jain, J., Loh, C., and Rao, A. (1995) Transcriptional regulation of the IL-2 gene. *Curr. Opin. Immunol.* **7,** 333–342
36. Su, B., Jacinto, E., Hibi, M., Kallunki, T., Karin, M., and Ben Neriah, Y. (1994) JNK is involved in signal integration during costimulation of T lymphocytes. *Cell* **77,** 727–736
37. Spiegel, S., and Merrill, A. H., Jr. (1996) Sphingolipid metabolism and cell growth regulation. *FASEB J.* **10,** 1388–1397
38. Dbaibo, G. S., Perry, D. K., Gamard, C. J., Platt, R., Poirier, G. G., Obeid, L. M., and Hannun, Y. A. (1997) Cytokine response modifier A (CrmA) inhibits ceramide formation in response to tumor necrosis factor (TNF)-alpha: CrmA and Bcl-2 target distinct components in the apoptotic pathway. *J. Exp. Med.* **185,** 481–490
39. Schutze, S., Potthoff, K., Machleidt, T., Berkovic, D., Wiegmann, K., and Krönke, M. (1992) TNF activates NF-κB by phosphatidylcholine-specific phospholipase C-induced 'acidic' sphingomyelin breakdown. *Cell* **71,** 765–776
40. Machleidt, T., Wiegmann, K., Henkel, T., Schütze, S., Baeuerle, P., and Krönke, M. (1994) Sphingomyelinase activates proteolytic I kappa B-alpha degradation in a cell-free system. *J. Biol. Chem.* **269,** 13760–13765
41. Yang, Z., Costanzo, M., Golde, D. W., and Kolesnick, R. N. (1993) Tumor necrosis factor activation of the sphingomyelin pathway signals nuclear factor kappa B translocation in intact HL-60 cells. *J. Biol. Chem.* **268,** 20520–20523
42. Ghosh, P., Sica, A., Cippitelli, M., Subleski, J., Lahesmaa, R., Young, H. A., and Rice, N. R. (1996) Activation of nuclear factor of activated T cells in a cyclosporin A-resistant pathway. *J. Biol. Chem.* **271,** 7700–7704
43. Pushkareva, M., Obeid, L. M., and Hannun, Y. A. (1995) Ceramide: an endogenous regulator of apoptosis and growth suppression. *Immunol. Today* **16,** 294–297
44. Ballou, L. R., Laulederkind, S. J. F., Rosloniec, E. F., and Raghow, R. (1996) Ceramide signalling and the immune response. *Biochim. Biophys. Acta* **1301,** 273–287
45. Tokura, Y., Wakita, H., Yagi, H., Nishimura, K., Furukawa, F., and Takigawa, M. (1996) Th2 suppressor cells are more susceptible to sphingosine than Th1 cells in murine contact photosensitivity. *J. Invest. Dermatol.* **107,** 34–40
46. Sakano, S., Takemura, H., Yamada, K., Imoto, K., Kaneko, M., and Ohshika, H. (1996) Ca^{2+} mobilizing action of sphingosine in Jurkat human leukemia T cells. Evidence that sphingosine releases Ca^{2+} from inositol trisphosphate- and phosphatidic acid-sensitive intracellular stores through a mechanism independent of inositol trisphosphate. *J. Biol. Chem.* **271,** 11148–11155
47. Hashizume, T., Kageura, T., and Sato, T. (1998) Different effects of cell-permeable ceramide analogs on platelet activation. *Biochem. Mol. Biol. Int.* **44,** 489–496
48. Burleigh, B. A., and Andrews, N. W. (1998) Signaling and host invasion by *Trypanosoma cruzi*. *Curr. Opin. Microbiol.* **1,** 461–465
49. Michel, C., and van Echten Deckert, G. (1997) Conversion of dihydroceramide to ceramide occurs at the cytosolic face of the endoplasmic reticulum. *FEBS Lett.* **416,** 153–155
50. Olivera, A., Zhang, H., Carlson, R. O., Mattie, M. E., Schmidt, R. R., and Spiegel, S. (1994) Stereospecificity of sphingosine-induced intracellular calcium mobilization and cellular proliferation. *J. Biol. Chem.* **269,** 17924–17930
51. Xavier, M. T., Previato, J. O., Andrade, A. F. B., and Mendonça-Previato, L. (1991) Evidence for the presence of β-D-galactofuranosyl residues (1–3)-linked to α-D-mannopyranose on the cell membrane in all development stages of *Trypanosoma cruzi*. *Ci. Cult. J. Braz. Assoc. Adv. Sci.* **43,** 49
52. Golgher, D. B., Colli, W., Souto-Padron, T., and Zingales, B. (1993) Galactofuranose-containing glycoconjugates of epimastigote and trypomastigote forms of Trypanosoma cruzi. *Mol. Biochem. Parasitol.* **60,** 249–264
53. Gottlieb, M. (1977) A Carbohydrate-containing antigen from *Trypanosoma cruzi* and its detection in the circulation of infected mice. *J. Immunol.* **119,** 465–470
54. Gottlieb, M. (1978) *Trypanosoma cruzi*: identification of a cell surface polysaccharide. *Exp. Parasitol.* **45,** 200–207
55. Minoprio, P., Itohara, Y., Heusser, C., Tonegawa, S., and Coutinho, A. (1989) Immunobiology of murine *T. cruzi* infection: the predominance of parasite-nonspecific responses and the activation of TCRI T cells. *Immunol. Rev.* **112,** 187–203
56. Lopes, M. F., da Veiga, V. F., Santos, A. R., Fonseca, M. E., and DosReis, G. A. (1995) Activation-induced CD4+ T cell death by apoptosis in experimental Chagas' disease. *J. Immunol.* **154,** 744–752
57. Freire-de Lima, C. G., Nunes, M. P., Corte-Real, S., Soares, M. P., Previato, J. O., Mendonça-Previato, L., and DosReis, G. A. (1998) Proapoptotic activity of a *Trypanosoma cruzi* ceramide-containing glycolipid turned on in host macrophages by IFN-γ. *J. Immunol.* **161,** 4909–4916

Received for publication November 17, 1998.
Revised for publication March 19, 1999.